

NATIONAAL LUCHT- EN RUIMTEVAARTLABORATORIUM

NATIONAL AEROSPACE LABORATORY NLR

THE NETHERLANDS

NLR TP 97374 U

COMPUTATION OF AIRCRAFT NOISE PROPAGATION
THROUGH THE ATMOSPHERIC BOUNDARY LAYER

by

J.B.H.M. Schulten

19980824 022



Reprints from this document may be made on condition that full credit is given to the Nationaal Lucht- en Ruimtevaartlaboratorium (National Aerospace Laboratory NLR) and the author(s).

NATIONAAL LUCHT- EN RUIMTEVAARTLABORATORIUM
NATIONAL AEROSPACE LABORATORY NLR



Anthony Fokkerweg 2, 1059 CM AMSTERDAM, The Netherlands
P.O. Box 90502 , 1006 BM AMSTERDAM, The Netherlands
Telephone : 31-(0)20-5 11 31 13
Fax : 31-(0)20-5 11 32 10

DOCUMENT CONTROL SHEET

	ORIGINATOR'S REF. TP 97374 U		SECURITY CLASS. Unclassified
ORIGINATOR National Aerospace Laboratory NLR, Amsterdam, The Netherlands			
TITLE Computation of aircraft noise propagation through the atmospheric boundary layer			
PRESENTED AT the Fifth International Congress on Sound and Vibration, University of Adelaide, Australia, Dec. 15-18, 1997			
AUTHORS J.B.H.M. Schulten		DATE 970730	pp ref 13 9
DESCRIPTORS Atmospheric boundary layer Doppler effect Eikonal equation Footprints Noise prediction (aircraft)			
Noise propagation Ray tracing Runge-Kutta method Sound pressure Wind velocity			
ABSTRACT Of all outdoor noise sources, aircraft probably have the largest impact on communities. As a result, the accurate prediction of aircraft noise exposure is of great interest. Nevertheless, conventional procedures for quantifying aircraft noise draw heavily on empirical data in which source and propagation effects are more or less statistically lumped together. A physically more relevant modeling of aircraft noise propagation is the ray acoustics approximation. Whereas ray acoustics techniques are well developed for stationary sources, they are not often applied to aircraft noise because the aircraft motion in principle requires many time-consuming computations to obtain the time history of a single takeoff or landing event. The present paper describes the application of the method of ray-tracing to a source moving along a three-dimensional path in a realistic atmosphere. The method is illustrated by typical examples of the effects of a non-uniform wind and temperature profile such as the formation of acoustic shadow zones without any noise and, alternatively, zones with multiple reflections. It is shown that large reductions in computation time can be obtained if the flight path is close to level, which is factual for the majority of civil aircraft movements.			



NLR TECHNICAL PUBLICATION
TP 97374 U

COMPUTATION OF AIRCRAFT NOISE PROPAGATION
THROUGH THE ATMOSPHERIC BOUNDARY LAYER

by
J.B.H.M. Schulten

The contents of this report have been initially prepared for publication as paper 389438 in the Proceedings of the Fifth International Congress on Sound and Vibration, University of Adelaide, Australia, Dec. 15-18, 1997.

This investigation has been carried out under a contract awarded by the Netherlands Agency for Aerospace Programs, contract number 01607N.

Division : Fluid Dynamics
Prepared : JBHMS/ 
Approved : HHB/ 

Completed : 980402
Order number: 101.661
Typ. : JBHMS



Contents

ABSTRACT	5
INTRODUCTION	5
ANALYSIS	6
NUMERICAL IMPLEMENTATION	8
Integration algorithm	8
Wind velocity profile	8
Temperature profile	9
Reflection at the ground surface	9
Doppler effect	11
SINGLE-EVENT TIME HISTORY	12
CONCLUDING REMARKS	13
REFERENCES	13

4 Figures



This page is intentionally left blank.



COMPUTATION OF AIRCRAFT NOISE PROPAGATION THROUGH THE ATMOSPHERIC BOUNDARY LAYER*

Johan B.H.M. Schulten

National Aerospace Laboratory NLR, Aeroacoustics Department, the Netherlands

ABSTRACT

Of all outdoor noise sources, aircraft probably have the largest impact on communities. As a result, the accurate prediction of aircraft noise exposure is of great interest. Nevertheless, conventional procedures for quantifying aircraft noise draw heavily on empirical data in which source and propagation effects are more or less statistically lumped together. A physically more relevant modeling of aircraft noise propagation is the ray acoustics approximation. Whereas ray acoustics techniques are well developed for stationary sources, they are not often applied to aircraft noise because the aircraft motion in principle requires many time-consuming computations to obtain the time history of a single takeoff or landing event. The present paper describes the application of the method of ray-tracing to a source moving along a three-dimensional path in a realistic atmosphere. The method is illustrated by typical examples of the effects of a non-uniform wind and temperature profile such as the formation of acoustic shadow zones without any noise and, alternatively, zones with multiple reflections. It is shown that large reductions in computation time can be obtained if the flight path is close to level, which is factual for the majority of civil aircraft movements.

INTRODUCTION

Despite very significant noise reductions on the individual jet aircraft over the last 30 years, the continuous growth of air transportation goes together with an increasing concern about the community noise. Although some noise can sometimes be heard in quiet areas from *en route* aircraft at cruising altitude, by far the most noise is heard in the vicinity of airports. Since airports are necessarily in the neighborhood of concentrations of people, the solution of the problem will always remain a compromise. In order to make noise forecasts, it is not only necessary to have detailed information on the noise emitted by the aircraft during take off and landing. Also the trajectory of the aircraft plays an important role and gives, within limitations of aircraft traffic control and safety, possibilities to minimize the population affected by the noise. To assess the actual noise level eventually observed on the ground, propagation through the atmosphere plays a crucial role. In the present paper the latter aspect is addressed. Conventional, empirical methods to calculate community noise do not consider atmospheric conditions in detail. It will appear that it is not sufficient to average atmospheric conditions over longer periods and that only the actual conditions can give the relevant result. In particular the wind direction has a very large effect on the noise impact. At frequencies typical of aircraft noise (1 - 3 kHz) the ray acoustics approximation is valid. For stationary, ground based sources, ray acoustics is a well-developed technique, e.g.

* Supported by the Netherlands Agency for Aerospace Programs (NIVR), Contract 01607N.



Lamancusa and Daroux [1]. For aircraft, with their continuously changing position, the ray acoustics computations seem, at first sight, to be too time consuming for practical purposes. Although this may be true for agilely manoeuvring military aircraft, it will be shown that for the more uniformly moving civil aircraft computation is quite feasible.

ANALYSIS

For high frequency aircraft noise the atmospheric wind velocity w and speed of sound c can be considered as locally constant on the scale of the typical wavelength. Then, the sound field pressure satisfies the convective-wave equation

$$\nabla^2 p - \frac{1}{c^2} \left[\frac{\partial^2 p}{\partial t^2} + 2(w \cdot \nabla) \frac{\partial p}{\partial t} + (w \cdot \nabla)(w \cdot \nabla p) \right] = 0 \quad (1)$$

We now consider a single frequency ω and rewrite p as

$$p = P(x, \omega) \exp\{i\omega[t - \tau(x)]\} \quad (2)$$

to make the phase $(\omega\tau)$ explicit. Note that surfaces of constant phase are given by $t - \tau(x) = \text{constant}$. If we expand the (real) pressure amplitude into orders of the inverse frequency as follows

$$P(x, \omega) = P_0(x) + \frac{1}{\omega} P_1(x) + \frac{1}{\omega^2} P_2(x) + \dots \quad (3)$$

and substitute Eqs.(2) and (3) in the convected-wave equation [Eq.(1)], we obtain for the leading order (ω^2)

$$|\nabla\tau|^2 - \left[\frac{1 - w \cdot \nabla\tau}{c} \right]^2 = 0 \quad (4)$$

which is the eikonal equation for the case with a moving medium. Note that the amplitude P does not occur in this equation. The amplitude is governed by the next order (ω) equation

$$\nabla P_0 \cdot \left[\nabla\tau + w \frac{1 - w \cdot \nabla\tau}{c^2} \right] = -\frac{P_0}{2} \left[\nabla^2\tau - \frac{w \cdot (w \cdot \nabla)\nabla\tau}{c^2} \right] \quad (5)$$

Since higher orders of the amplitude will not be considered any further, the index of P_0 is suppressed in the sequel for brevity.

From now on we change our point of view to the larger atmospheric scale in which wind velocity w and speed of sound c are no longer constants. Application of the theory of characteristics, e.g. Bleistein [2], yields the first ray tracing equation for the normal on the wave fronts $\nabla\tau$ which will be denoted by q in the following vector equation

$$\frac{dq}{dt} = -|q| \nabla c - q \times (\nabla \times w) - (q \cdot \nabla) w \quad (6)$$

where t is the time traveled along the ray (=characteristic). In more lucid, Cartesian components the equation reads

$$\begin{aligned}\frac{dq_x}{dt} &= -|q| \frac{\partial c}{\partial x} - q \cdot \frac{\partial w}{\partial x} \\ \frac{dq_y}{dt} &= -|q| \frac{\partial c}{\partial y} - q \cdot \frac{\partial w}{\partial y} \\ \frac{dq_z}{dt} &= -|q| \frac{\partial c}{\partial z} - q \cdot \frac{\partial w}{\partial z}\end{aligned}\tag{7}$$

Similarly, the position of the ray in space is governed by the second ray tracing equation

$$\frac{dx}{dt} = c \frac{q}{|q|} + w\tag{8}$$

For a stratified atmosphere, i.e. one in which w and c depend only on the altitude and w is horizontal, Eq.(5) can be rewritten as

$$\nabla \cdot \left\{ P^2 \left[q + w \frac{1 - w \cdot q}{c^2} \right] \right\} = 0\tag{9}$$

The common way to solve for the pressure amplitude is to apply Gauss' divergence theorem to Eq.(9) and find the relation of the amplitude to the cross area of the ray tubes made up by adjacent rays. Another, similar way is to use Blokhintshev's invariant, e.g. Pierce [3]. The disadvantage of this approach for practical purposes is that we have to translate this geometrical construction into computational statements that involve subtractions of the kind that lead to serious loss of numerical accuracy. To make things worse: these problems are the most severe in areas where adjacent rays tend to intersect and amplitudes tend to infinity (caustics). Therefore, we will follow a different approach in which the critical numerical manipulations are replaced by analytical operations.

Along a ray we have

$$\nabla P \cdot \frac{dx}{dt} = \frac{dP}{dt}\tag{10}$$

Substitution of Eq.(8) in Eq.(10) yields

$$\frac{dP}{dt} = \nabla P \cdot \left[c \frac{q}{|q|} + w \right]\tag{11}$$

Finally, substitution of the eikonal equation in the left hand side of Eq.(5) leads to the amplitude evolution equation

$$\frac{dP}{dt} = \frac{P}{2|q|} \left[\frac{w \cdot (w \cdot \nabla) q}{c} - c \nabla \cdot q \right]\tag{12}$$

Similar ideas have been developed by Chen and Ludwig [4] and Colonius et al.[5], but they prefer a local ray-coordinate system to describe the derivatives normal to the rays. The right hand side of Eq.(12) contains spatial derivatives of q . These are obtained by differentiating the components of dq/dt in Eq.(7). For instance,



$$\frac{d}{dt} \frac{\partial q_x}{\partial z} = - \left[\frac{\partial |q|}{\partial z} \frac{\partial c}{\partial x} + |q| \frac{\partial^2 c}{\partial x \partial z} + \frac{\partial q}{\partial z} \cdot \frac{\partial w}{\partial x} + q \cdot \frac{\partial^2 w}{\partial x \partial z} \right] \quad (13)$$

As a result we need to integrate 7 additional evolution equations [6 derivatives + Eq.(12)] to obtain the amplitude along a ray.

NUMERICAL IMPLEMENTATION

Integration algorithm

Mathematically, the problem to be solved is an initial value problem of a system of 16 first order, ordinary differential equations. In the present study the integration in time of these equations is performed by a 4th-order Runge-Kutta method with adaptive time step size, e.g. Press et al.[6]. Initial values are given on the surface of a sphere with a finite radius and the integration is marched until a certain time has been attained, typically 30 seconds which is enough to cover a distance of about 10 km from the source. For simplicity, in the present study an SPL of 130 dB on a sphere with a 1 m radius has been taken, but in practical calculations the aircraft noise directivity pattern should be applied here.

In principle, the atmospheric absorption of sound can be directly implemented in the amplitude evolution Eq.(12). In the present basic study atmospheric absorption is not further considered but formulae for atmospheric absorption including the effects of humidity and frequency can be found in Bass et al.[7].

Wind velocity profile

Of all atmospheric effects, the wind velocity variation has the largest effect on sound propagation. The atmospheric wind velocity is for most purposes adequately described by a logarithmic profile, in which the singular point is just below the zero ground level. This nearly singular behavior is not only nonphysical, it also forces the numerical integration to take very small steps which result in long computing times. In reality the turbulent boundary layer has a sublayer close to the ground where it has to satisfy the so-called laws of the wall. These require the 2nd and 3rd order normal derivatives to vanish at the wall. To this end Reichardt [8] proposed the following, experimentally validated, turbulent boundary layer profile

$$w = w_{\tau_0} \left[\frac{1}{K} \ln(1 + \bar{z}) + C \left[1 - \exp\left[-\frac{\bar{z}}{\alpha}\right] - \frac{\bar{z}}{\alpha} \exp[-\beta \bar{z}] \right] \right] \quad (14)$$

where w_{τ_0} is the shear stress velocity at the ground surface, $K=0.4$ (von Kármán's constant for turbulent boundary layers), $C = 7.4$, $\alpha = 11.0$, $\beta = 0.33$. In the present study, this wind profile is adapted for a rough surface by scaling the vertical coordinate \bar{z} on the roughness height of the ground. A roughness height typical for the surroundings of airports of 0.15m has been adopted in the numerical examples.

In Fig.1 rays emitted from a source in a wind velocity of 7 m/s (at 10 m height) are shown. Upstream rays are bent upward and yield a zone of silence beyond 2 km upstream. Downstream rays are bent downward by wind refraction and some of them are multiply reflected.



Temperature profile

In the standard atmosphere the temperature decreases with height as $T = 288.16 - 0.0065 z$. The most important effect of the temperature is its relation with the speed of sound which is proportional to the square root of the temperature. This neutral equilibrium temperature distribution has some beneficial effect since sound rays will be bent upward by a decreasing speed of sound. This effect can be observed in Fig.1 for the rays emitted downstream.

While neutral equilibrium is the usual temperature distribution in the presence of wind, a different situation can occur at night when a layer of cool air is formed near the ground in still air. Such an inversion can have an adverse effect on the sound impact of sources below the inversion point (typically 100-200m) like aircraft taking off in the early morning.

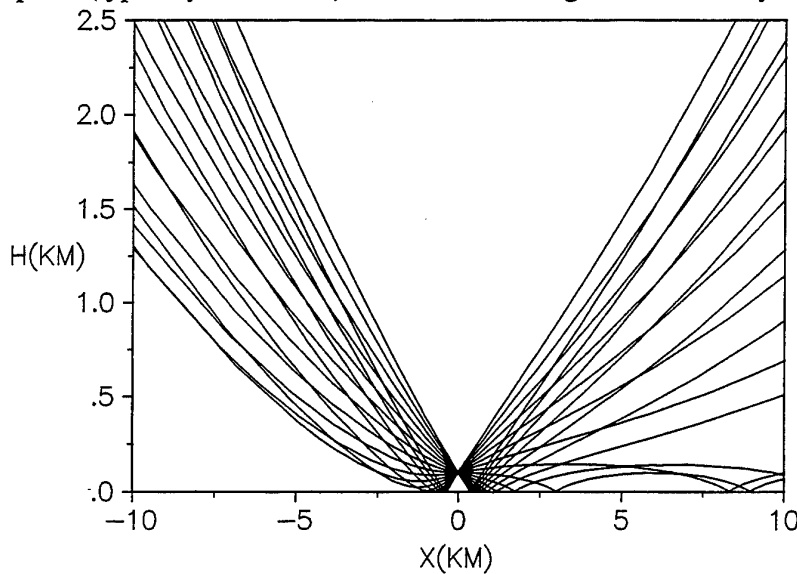


Fig.1 Rays from a source at 100 m altitude

Reflection at the ground surface

The standard way to measure aircraft noise on the ground is by a microphone at a height of 1.2 m above the ground level. Therefore in almost all cases the measured sound is made up by directly incident rays and ground reflected rays. In ray acoustics, ground reflection can be modeled in a quite straightforward way; the wave fronts are reflected by a change of sign of the following quantities at $z=0$:

$$q_z, \frac{\partial q_x}{\partial z}, \frac{\partial q_y}{\partial z}, \frac{\partial q_z}{\partial x}, \frac{\partial q_z}{\partial y}, \frac{\partial q_z}{\partial z} \quad (15)$$

For a perfectly hard surface the amplitude and phase remain unaltered by reflection. However, in general the surface of the ground will be acoustically soft, which can be modeled by a ground impedance. Impedance data for grass-covered ground, which have been used in the present paper, are given by Donato [9].



The (complex) reflection coefficient for a surface with normalized ground impedance Z is given by

$$R = \frac{\sin\phi - 1/Z(\omega)}{\sin\phi + 1/Z(\omega)} \quad (16)$$

where ϕ denotes the incident (grazing) angle and $\sin\phi = -q_z/|q|$.

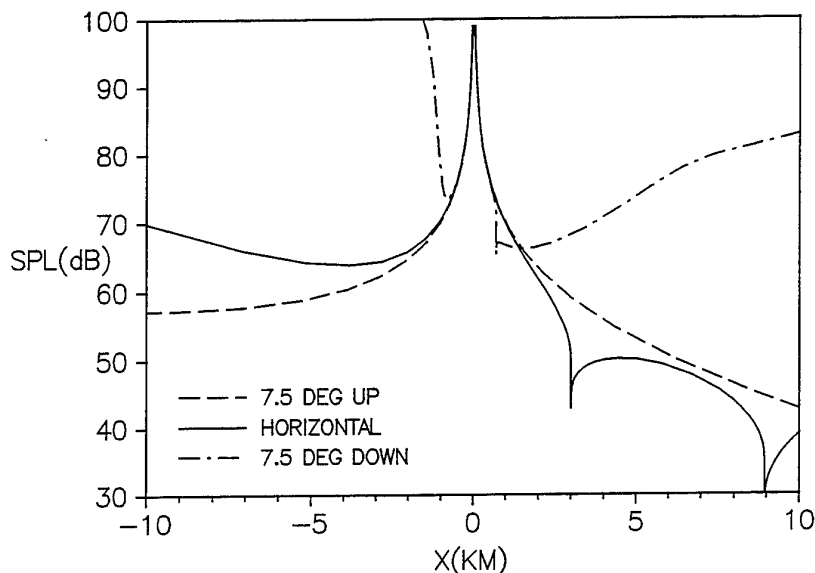


Fig.2 Ray sound pressure level for different emission angles

Fig.2 gives the sound pressure level along some of the rays shown in Fig.1. The rays emitted at positive angles of 7.5 deg show a fairly simple behavior in which the relatively higher level of the upstream ray can be clearly observed. The forward ray emitted horizontally has a gradually increasing level as it approaches the caustic which forms the boundary of the zone of silence. This effect is much stronger for the ray emitted at a downward angle of 7.5 deg. This ray almost coincides with the caustic and shows an extremely rapidly growing amplitude after passage of its turning point. To avoid numerical overflow, the computer program tempers the growth by clipping the amplitude at 10 times its value for the corresponding arc length traveled along the ray in a uniform atmosphere. Fortunately, the major part of the exceptional amplitude growth takes place at higher altitudes than ground observation level. Nevertheless, it is a shortcoming of the present method that a proper treatment of the caustic, e.g. Pierce [3], has not yet been incorporated. The ray emitted horizontally in the downstream direction has two ground reflections. It is quite remarkable how the amplitude drops as the ray approaches the ground and restores while going upward after reflection. Finally, the ray emitted downstream at an angle of 7.5 deg toward the surface clearly shows the sudden amplitude drop at the reflection point. After reflection, the opposed effects of natural spreading and wind refraction are clearly observed.

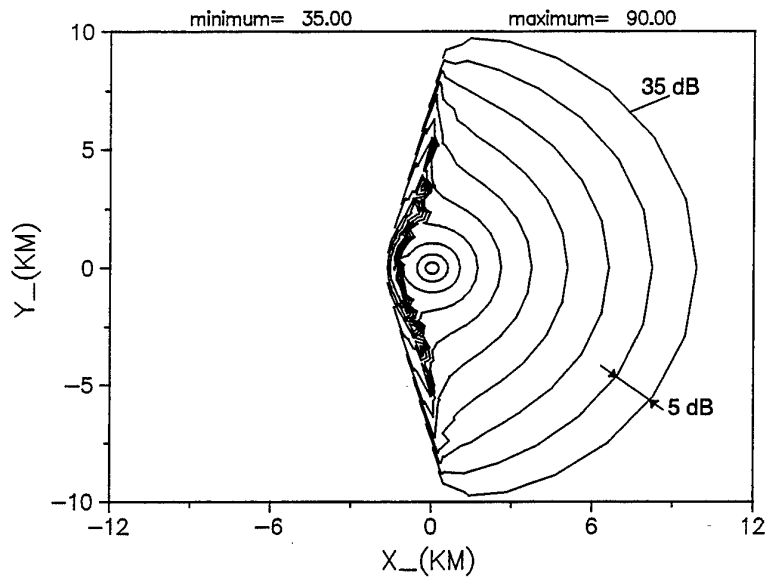


Fig.3 Sound pressure level at microphone height 1.2 m of a source at 300 m altitude. Intervals of 4 dB between contour lines. Wind velocity 7 m/s at 10 m height.

In Fig.3 an x,y surface contour plot is given of the sound pressure level at standard microphone height for a source at 300 m altitude. Like in the previous figures, the wind velocity is 7 m/s at a height of 10 m. This kind of 'footprints' forms the basis from which the variation in time of the pressure amplitude caused by an aircraft passage can be computed. While in the downstream half the spherical spreading of the sound is easily recognized, in the upstream half the picture is completely deformed by the zone of silence and the adjacent caustic surface. The footprint shows why one can not use a wind direction averaged over a long period since this would predict an unrealistic permanent zone of silence.

Doppler effect

One of the characteristics of aircraft noise is the motion of the source. A consequence of this motion is the fact that the frequency of the sound heard by stationary observers depends on the emission angle from the source. For a typical Mach number of 0.3 and a source frequency of 1000 Hz the frequency heard on the ground varies from 1430 Hz to 770 Hz during a fly-over. The frequency ω of the sound in the stationary field is related to the frequency ω_0 in the moving source system as, e.g. Pierce, Ch.9 [3]

$$\omega = \frac{\omega_0}{1 - \frac{\mathbf{v} \cdot \mathbf{q}_0}{c |\mathbf{q}_0|}} \quad (17)$$

where \mathbf{v} is the source velocity and the subscript 0 relates to the conditions at emission. Once again, it is noted that the ray-acoustics theory can incorporate the Doppler effect perfectly. The fact that each ray has a different frequency does not add any complexity to the calculation.



SINGLE-EVENT TIME HISTORY

The ultimate goal of the aircraft noise calculations is to assess the community noise load for any point of interest at the ground. Physically this means that we have to calculate the variation of the sound pressure level and frequency in time for a single aircraft passage and to repeat this of course many times. Nevertheless, the single-event time history is the crucial element in the composition of the noise load over longer periods.

Let us, for a start, assume an aircraft flying horizontally with a constant velocity at height Z . Then, it is not difficult to see that the sound amplitude recorded by a microphone is related to the footprint level computed thus far as follows

$$P_{mic}(x,y,t) = P_f[x-v_x t, y-v_y t, Z] \quad (18)$$

Here, P_f is to be understood as the SPL measured at microphone level from a source at altitude Z . The main work to be done is a two-dimensional interpolation between the points in the footprint and the microphone time.

A more general situation is the case for which the vertical speed is not zero but still considerably smaller than the horizontal flight speed. Then it is no longer sufficient to have only a footprint for one aircraft altitude but we need at least 2 footprints to be able to interpolate also for the source height. Since the pressure amplitude due to the upwind caustic has a rather discontinuous behavior, interpolation is delicate.

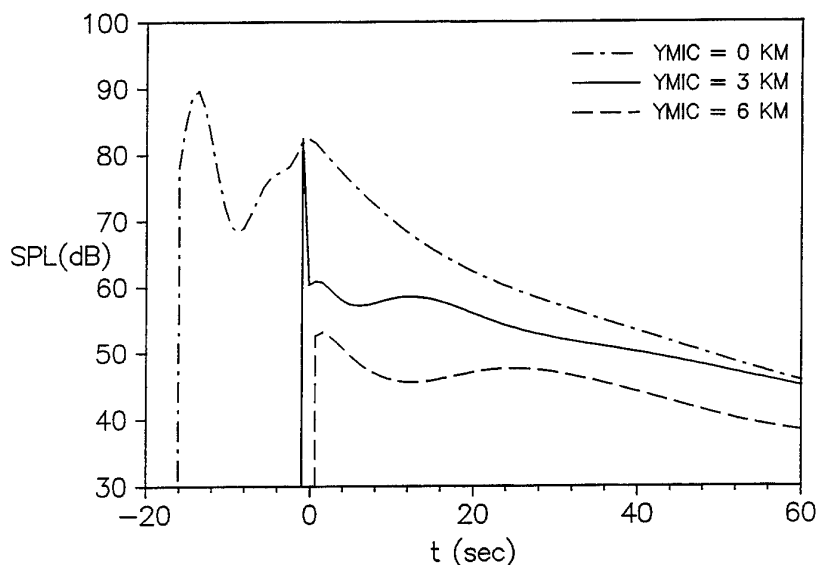


Fig.4 SPL time history of a fly-over at 300 m altitude: 3 lateral microphone positions.

The amplitude is now computed from

$$P_{mic}(x,y,t) = P_f[X, Y, Z_1] + (Z(t)-Z_1) \frac{P_f[X, Y, Z_2] - P_f[X, Y, Z_1]}{Z_2 - Z_1} \quad (19)$$

with



$$X = x - \int_0^t v_x(t') dt', \quad Y = y - \int_0^t v_y(t') dt'$$

By virtue of the interpolation, it is now even possible to accommodate variations in aircraft speed, engine RPM etc. between the two altitudes Z_1 and Z_2 , as long as these variations are slow in relation to the sound wavelength, just as the variation in wind velocity and temperature. This will be the case in almost every practical situation.

As an example Fig.4 shows the SPL time history for a horizontal fly-over at three observation points constructed from the footprint of Fig.3. The sudden rise from silence to a very loud level is observed at all three lateral positions but the shape of the time history very much depends on the lateral position. The extremely sharp peak for the 3 km position will almost certainly be reduced by a more complete physical modeling of the acoustic behavior near the caustic.

CONCLUDING REMARKS

A ray acoustics method to compute atmospheric effects on aircraft noise propagation has been discussed. Instead of using the concept of ray tubes, an alternative way to compute the amplitude simultaneously with the ray trajectory itself has been applied.

Wind refraction proves to be a very substantial atmospheric propagation effect by creating zones of silence as well as fronts of extreme amplitude (caustics).

The fairly uniform motion of civil aircraft allows large steps in interpolation of footprints to save considerable computing time in the construction of single-event time histories.

REFERENCES

1. Lamancusa, J.S., Daroux, P.A., "Ray tracing in a moving medium with two-dimensional sound-speed variation and application to sound propagation over terrain discontinuities", *J. Acoust. Soc. Am.*, Vol.93, No.4, Pt.1, April 1993, pp. 1716-1726.
2. Bleistein, N., *Mathematical Methods of Wave Phenomena*, Academic Press, Orlando, 1984.
3. Pierce, A.D., *Acoustics - An Introduction to Its Physical Principles and Applications*, McGraw-Hill, New York, 1981.
4. Chen, K.C., Ludwig, D., "Calculation of wave amplitudes by ray tracing", *J. Acoust. Soc. Am.*, Vol.54, No.2, 1973, pp.431-436.
5. Colonius, T., Lele, S.K., Moin, P., "The scattering of sound waves by a vortex: numerical simulations and analytical solutions", *J. Fluid Mech.*, Vol.260, 1994, pp.271-298.
6. Press, W.H., Flannery, B.P., Teukolsky, S.A., Vetterling, W.T., *Numerical Recipes*, Cambridge University Press, Cambridge, 1989.
7. Bass, H.E., Sutherland, L.C., Zuckerwar, A.J., "Atmospheric absorption of sound: Update", *J. Acoust. Soc. Am.*, Vol.88, Pt.4, Oct. 1990, pp.2019-2021.
8. Reichardt, H., "A Complete Description of the Turbulent Velocity Distribution in Smooth Ducts" (in German), *Z. angew. Math. Mech.* Vol.31, No.7, 1951, pp. 208-219.
9. Donato, R.J., "Impedance models for grass-covered ground", *J. Acoust. Soc. Am.*, Vol.61, No.6, June 1977, pp.1449-1452.